In vitro and in vivo 19-Fluorine Magnetic Resonance Imaging (MRI) of β-cells and pancreatics using GLUT-2 specific contrast agents

Sayuan Liang[1], Hauke Kolster[1], Karim Louchami[2], Tom Dresselaers[1], Willy Malaisse[2], Sonu Sharma[1], and Uwe Himmelreich[1]
[1]*Biomedical MRI unit/MoSAIC, Department of Imaging and Pathology, K.U.Leuven, Leuven, Belgium,* [2]*Laboratory of Experimental Hormonology, Université Libre de Bruxelles, Bruxelles, Belgium*

Introduction

The assessment of the β-cell mass in experimental models of diabetes and ultimately in patients is a hallmark to understand the relationship between reduced β-cell mass/function and the onset of diabetes. Several attempts have been made to visualize β-cells in vivo using targeted nanoparticles and MRI. However due to the small size of fenestra in pancreatic islets, not all β-cells can be reached, preventing quantitative assessment of β-cell mass. ^{19}F MRI has emerged as a new alternative method for MRI cell tracking [1] because it provides potential non-invasive localization and quantification of labeled cells. The purpose of this project is to validate β-cell and pancreatic islet imaging by using fluorinated, GLUT-2 targeting mannoheptulose derivatives (FMH) in vivo. It has been shown before that the GLUT-2 transporter is highly expressed in both β-cells and hepatocytes and that mannoheptulose has high uptake specificity for the GLUT-2 transporter [2-4].

Methods

Contrast agent: 1-FMH; 3-FMH and 1,3-FMH were synthesized according to [3]. β-cells like cells (INS-1), mouse hepatocytes, fibroblasts (negative controls) and rat pancreatic islets were labeled with the three FMH derivatives by overnight culture. Cell viability, cell function (insulin production) and ^{19}F-MRI detectability were validated.

In vivo experiments: In vivo ^{19}F MRI was performed after systemic administration of 300 µl of 1-FMH or 3-FMH (each 200 mM solution), respectively. Hereby, male BL6 mice (body weight 25g) were anesthetized using isoflurane. Organs (muscle, bladder, kidney, liver, and pancreas) were removed after the final MRI scan for quantification by high-resolution ^{19}F NMR spectroscopy using the homogenized tissue.

^{19}F-MRI/ NMR: All MRI experiments were performed using a 9.4T Biospec small animal MRI system (Bruker, Ettlingen, Germany). For phantom experiments on cell suspensions, a purpose-build transmit-receive solenoid coil with an inner diameter of 4 cm and tunable to the ^{1}H (400.34 MHz) and ^{19}F (376.64 MHz) was used. For all in vivo experiments, a single loop, saddle-shape surface coil (42 mm x 66 mm) was built to allow whole body mouse imaging. Phantom studies (agar gel containing different concentrations of perfluorocrown ethers) were performed to determine the profile of the coil. Both in vivo ^{1}H and ^{19}F MR images were obtained immediately after injection of FMH using a multi-slice (10 x 2.5 mm slices) fast spin echo sequence with TE = 15.9ms; TR = 1000ms; FOV = 8cm x 4cm, and matrix = 100 x 50 (scan time is about 90 minutes). One mouse had a follow-up scan at 24 hours. Other animals were sacrificed immediately after the first imaging session (2 to 5 hours after the first FMH injection). The pixel-wise ^{19}F signal was considered significant if larger than 2*SD of background noise ($p<0.025$) at post-processing stage. ^{19}F NMR spectra of homogenized tissue samples were acquired by using a vertical NMR spectrometer (Bruker Avance II, 9.4T) after addition of a known concentration of 5-FC as an external concentration and chemical shift reference.

Results & Discussion

Uptake of 1-FMH, 3-FMH and 1,3-FMH was specific to cells expressing the GLUT-2 transporter. Intracellular concentrations were highest for INS-1 cells and pancreatic islets (15-20mM) followed by hepatocytes (8-12mM). Cell survival was not affected by labeling with the FMH derivatives. However, insulin secretion after stimulation with 10mM glucose was inhibited by 20% (3-FMH) up to 40% (1,3-FMH) [2]. In vitro experiments allow detection of down to 1000 cells μl^{-1}.

The profile of the purpose built coil for in vivo studies was determined using a phantom, which indicated similar profiles for both ^{19}F and ^{1}H imaging thus facilitating overlay of images and interpretation of the localization of the contrast agents (labeled cells).The linear relationship between ^{19}F concentration and ^{19}F signal intensity makes quantification feasible. The detection limit of this coil, defined as the number of atoms that result in an image with SNR of 5, is achieved with a concentration of $1.5*10^{16}$ F atoms/voxel (Flash 3D scan, resolution = 0.938mm x 0.938mm x 0.938mm, scan time = 45 minutes) which is comparable with other surface coils that have been used in published papers [5-6]. In-vivo images (Fig. 1) show clear signal from bladder, kidney, liver and potentially from the pancreas. Repeated MRI scans indicate rapid clearance of 1-FMH and 3-FMH from the circulation (kidney, bladder) and only low retention in the liver and pancreas. MRS of excited tissue confirms the presence of ^{19}F FMH in these organs (1-5 mM). Both in vivo MRI and in vitro MRS show almost complete clearance of ^{19}F FMHs 24 hours after injection.

Conclusions

We confirmed specific uptake of fluoromannoheptuloses via the GLUT-2 transporter in isolated β-cell lines, hepatocytes and pancreatic islets. We have established a set-up (^{19}F coil, acquisition protocol) for the detection of signals from ^{19}F compound in the mouse abdomen at the respective fluorine concentrations. In vivo experiments using the different FMH derivatives indicate rapid clearance of the compound via the kidney and bladder. While the FMH signal remaining in the liver and pancreas is potentially sufficient for in vivo β-cell and hepatocyte imaging, the sensitivity (for example by introducing more equivalent ^{19}F-atoms) has to be improved for applications in models of diabetes.

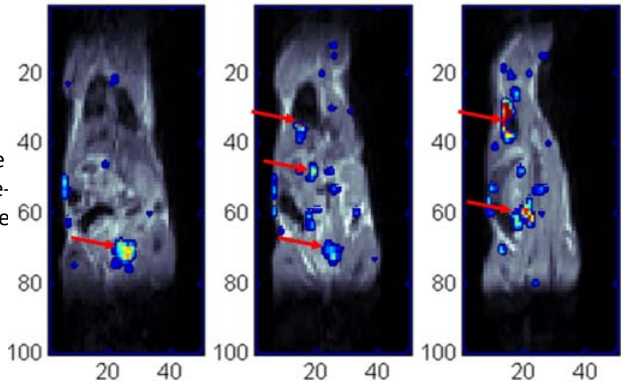

Figure 1.Three ^{1}H slices are overlaid with corresponding ^{19}F signal (Jet scale)

Reference

(1) Ahrens E et al. (2005) Nat Biotech 23: 983-987; (2) Malaisse WJ et al. (2012) Arch Biochem Biophys, 517(2), 138-43; (3)Waschke D et al. (2012) Eur.J.Org.Chem, 5, 948-59; (4)Himmelreich U et al. (2011) Met.Funct.Res.Diab, 3, 25(A19); (5)Boehm-Sturm P et al. (2011) PLoS One, 6(12): e29040; (6)Bonetto F et al. (2011) Int J Cancer, 129(2): 365-73.